Technical Report #53

AD-A205 688

REPORT DOCUMENTATION PAGE

1a. SECURITY CLASSIFICATION AUTHORITY NA	1b. RESTRICTIVE MARKINGS NA
2b. DECLASSIFICATION / DOWNGRADING SCHEDULE NA	3. DISTRIBUTION / AVAILABILITY OF REPORT Distribution Unlimited; Approved for Public Release
4. PERFORMING ORGANIZATION REPORT NUMBER(S)	5. MONITORING ORGANIZATION REPORT NUMBER(S) NA
6a. NAME OF PERFORMING ORGANIZATION Indiana University	6b. OFFICE SYMBOL (If applicable) NA
6c. ADDRESS (City, State, and ZIP Code) Department of Chemistry Bloomington, IN 47405	7a. NAME OF MONITORING ORGANIZATION ONR
8a. NAME OF FUNDING / SPONSORING ORGANIZATION	8b. OFFICE SYMBOL (If applicable)
8c. ADDRESS (City, State, and ZIP Code)	7b. ADDRESS (City, State, and ZIP Code) 800 N. Quincy Street Arlington, VA 22217
	9. PROCUREMENT INSTRUMENT IDENTIFICATION NUMBER Contract N00014-86-K-0366
	10. SOURCE OF FUNDING NUMBERS

PROGRAM ELEMENT NO.	PROJECT NO.	TASK NO.	WORK UNIT ACCESSION NO.
		R&T Code 4134006	

11. TITLE (Include Security Classification) Use of a Spectrally Segmented Photodiode-Array Spectrometer for Indictively Coupled Plasma Atomic Emission Spectroscopy

12. PERSONAL AUTHOR(S)
K.R. Brushwyler, N. Furuta, G.M. Hieftje

13a. TYPE OF REPORT	13b. TIME COVERED	14. DATE OF REPORT (Year, Month, Day)	15. PAGE COUNT
Technical	FROM _____ TO _____	February 10, 1989	27

16. SUPPLEMENTARY NOTATION

17. COSATI CODES		
FIELD	GROUP	SUB-GROUP

18. SUBJECT TERMS (Continue on reverse if necessary and identify by block number)
Inductively Coupled Plasma, Photodiode Array Spectrometer, Multielement Analysis. (mgn)

19. ABSTRACT (Continue on reverse if necessary and identify by block number)

The utility of a spectrally segmented photodiode array spectrometer was examined by using inductively coupled plasma atomic emission spectrometry (ICP-AES). The spectrometer used in this study is capable of high resolution (reciprocal linear dispersion of approximately 0.08 nm/mm at 300 nm) over a wide spectral range (190-415nm). The effect of using spectral-peak areas instead of peak heights as a signal definition was determined by using the emission signals from 10 molybdenum lines obtained at various photodiode-array integration periods. In addition, a signal definition involving a summation over a range of 5 pixels offered the best signal-to-noise ratio when the noise was defined as the standard deviation of the residual values from the line fit to the sideband background level. A detection limit of 6 ng/ml was determined in this way for molybdenum. The multichannel capability of the spectrometer was found to permit continuous background correction, thereby reducing errors caused by low-frequency noise or plasma drift. Detector linearity was found to extend over three orders of magnitude with a single integration period. However, by utilizing different integration periods, the linear range of the

(over)

20 DISTRIBUTION / AVAILABILITY OF ABSTRACT	21 ABSTRACT SECURITY CLASSIFICATION
☒ UNCLASSIFIED/UNLIMITED ☐ SAME AS RPT ☐ DTIC USERS	Distribution Unlimited

22a NAME OF RESPONSIBLE INDIVIDUAL	22b TELEPHONE (Include Area Code)	22c OFFICE SYMBOL
Gary M. Hieftje	(812) 335-2189	

DD FORM 1473, 84 MAR — 83 APR edition may be used until exhausted. All other editions are obsolete.

SECURITY CLASSIFICATION OF THIS PAGE

UNCLASSIFIED

Use of a Spectrally Segmented Photodiode-Array Spectrometer for Inductively Coupled Plasma Atomic Emission Spectroscopy

Examination of Procedures for the Evaluation of Detection Limits.

K.R. Brushwyler, N. Furuta[†], and G.M. Hieftje[††]
Department of Chemistry, Indiana University
Bloomington, IN 47405

[†] On leave from The National Institute for Environmental Studies
16-2 Onogawa, Tsukuba, Ibaraki 305, Japan.

[††] Corresponding author

Summary

The utility of a spectrally segmented photodiode array spectrometer was examined by using inductively coupled plasma atomic emission spectrometry (ICP-AES). The spectrometer used in this study is capable of high resolution (reciprocal linear dispersion of approximately 0.08 nm/mm at 300 nm) over a wide spectral range (190-415 nm). The effect of using spectral-peak areas instead of peak heights as a signal definition was determined by using the emission signals from 10 molybdenum lines obtained at various photodiode-array integration periods. In addition, a procedure to determine detection limits using such a spectrometer is proposed. It was found that a signal definition involving a summation over a range of 5 pixels offered the best signal-to-noise ratio when the noise was defined as the standard deviation of the residual values from the line fit to the sideband background level. A detection limit of 6 ng/ml was determined in this way for molybdenum. The multichannel capability of the spectrometer was found to permit continuous background correction, thereby reducing errors caused by low-frequency noise or plasma drift. Detector linearity was found to extend over three orders of magnitude with a single integration period. However, by utilizing different integration periods, the linear range of the detector could be extended to at least four orders of magnitude. The precision (RSD) of the spectrometer for a molybdenum concentration of 0.5 μg/ml was found to be about 3-4% for molybdenum peaks where the background emission was relatively low.

INTRODUCTION

Multichannel detectors such as vidicon tubes, linear photodiode arrays, and charge-transfer devices have been evaluated as detection systems for inductively coupled plasma atomic emission spectrometry (ICP-AES) [1-4]. Compared to photomultiplier-tube (PMT)-based detection systems, solid-state multichannel detectors are generally considered to be less sensitive to ultraviolet light and to suffer from either poor spectral resolution or limited spectral range. However, with the rapid development of solid-state technologies, the sensitivity of linear photodiode arrays has improved dramatically. Recently, a spectrally segmented photodiode-array spectrometer (Plasmarray®, LECO® Corporation) has been made commercially available for ICP-AES [5-7]. The unique optical arrangement of the spectrometer enables the simultaneous measurement of a number of emission lines over a wide spectral range (190-415 nm) while maintaining a high degree of spectral resolution. The spectrometer is easily reconfigured for the examination of different sets of spectral lines. As such, it is in essence a field-reprogrammable direct-reading spectrometer [5-7]. In the present study, several different definitions of noise and signal were examined, in order to establish realistic detection limits for the spectrometer. A total of ten molybdenum lines were measured. Because of the number and variety of molybdenum spectral lines that were investigated, the findings of this study can be extended to any spectral line when due consideration has been given to the definition of both the signal and the noise.

EXPERIMENTAL

Instrumentation

The linear-photodiode-array spectrometer used in this study has been discussed thoroughly in earlier papers [5-7] and will be described only briefly here. The optical system is shown schematically in Figure 1. The unique combination of wide spectral range and high resolution offered by this arrangement is derived from the combined use of three optical elements: a predispersion grating, an optical mask, and an Echelle grating. The source (an ICP was used in this study) is imaged by lens 1 onto a low-resolution (590 groves/mm) predispersion grating. The resulting dispersed light falls upon a demountable mask which has slots cut in it at positions corresponding to the elemental spectral lines of interest. The masks are designed and fabricated for specific sets of analytical lines and are readily interchanged. Light which is passed by slots in the optical mask is recollimated by mirror 1, "un-dispersed" by grating 2 and is incident upon an Echelle grating (31.6 grooves/mm, 63.5^{o} blaze angle) for final dispersion onto the photodiode array. The lack of a cross-dispersing element results in a spectrum at the photodiode array which represents the union of many orders from the Echelle grating. Accordingly, the spectral display is unconventional but elemental lines can be identified either by empirical calibration or computer modeling [5-7].

The mask used in this study was cut specifically for eleven molybdenum spectral lines and contained eleven slots. Table I relates the labeled spectral peak numbers in Figure 2d with the type of emission (i.e. ionic or atomic), the actual peak wavelengths, the grating order in which the dispersed spectral line falls, and the reciprocal linear dispersion at the location of incidence on the photodiode array. Figure 2 shows a series of spectra obtained with this mask. Spectrum a is a typical dark signal from the photodiode array. Spectrum b is a blank signal obtained from the continuous nebulization of water into an inductively coupled plasma. The dark signal shown in spectrum a has been subtracted from the signal obtained during the blank. Spectrum c is a dark-

subtracted spectrum showing the signal obtained from a 5 µg/ml solution of molybdenum. Spectrum d is the signal obtained by subtracting spectrum b from spectrum c.

The energy distribution of light incident upon the photodiode array in our prototype system is shown in Figure 3. The spectrum was obtained by removing the mask from the spectrometer. Although an ICP was used as the source in Figure 3, the complexity of the spectrum observed at the photodiode array without the mask in place produces a signal at the detector similar to that of a continuum. The attenuation of incident energy at higher pixel values is a result of slight differences between our Echelle grating and the one used in the original instrument design [5-7]. More recent spectrometer versions exhibit a flatter energy-response curve [8]. Because of the response of our present instrument (cf. Figure 3), only those lines incident upon the photodiode array at pixel values less than 600 were used in this study.

Operating parameters

The observation height in the ICP was fixed at 20 mm above the load coil, on the basis of visual observation of the emission from a 1000 µg/ml solution of Yttrium. Signal-to-noise ratios for the analytical lines of molybdenum were optimized by changing independently the plasma input power and the carrier-gas flow rate. The emission spectra obtained under optimal conditions for a) atomic emission and b) ionic emission are shown in Figure 4. The optimal conditions for atomic emission were an ICP power of 1.1 kW and a carrier (central) gas flow rate of 1.0 l/min. Throughout this study, the ICP was operated at conditions optimized for ionic emission, listed in Table II.

Experimental procedure

Because of the unconventional spectral presentation at the photodiode array, it is essential to define carefully both signal and noise in order to assign realistic detection limits for the spectrometer. Three different methods of determining noise were evaluated. First, a conventional approach was taken in which noise was defined as the standard deviation of ten independent

measurements on a blank solution at the spectral location of interest. For this definition of noise, the effect of integrating the signal over different numbers of pixels was examined. Thus, each spectral line was examined for signal definitions covering a range from 1 to 13 pixels, centered at the peak of the line (i.e. peak ±0 pixels, peak ±1 pixel, peak ±2 pixels,...,peak ±6 pixels). This procedure is illustrated in Figures 5a and 5b, which show signal and background definitions covering a five-pixel range. For each of these definitions, four different PDA integration times were examined: 10, 30, 50, and 100 seconds. For the definition of S and N, the detection limit, DL, for analyte x was defined in the conventional manner:

$$DL = 3(\sigma/S)[x] \qquad (1)$$

where σ is the standard deviation of the 10 blank solutions, and S is the average signal magnitude of 10 sample injections having an analyte concentration [x]. In addition to providing information regarding detection limits, these data helped evaluate the precision of the technique. For this latter portion of the study, a concentration of 0.5 μg/ml of molybdenum was used.

A second definition of noise involved utilizing the multichannel capability of the spectrometer to monitor simultaneously the signal and the surrounding background. By using this method (see Fig. 5c), selected regions on each side of a spectral line could be defined as the background. During data processing, a best-fit line was established for these background regions. This best-fit line represents the average baseline above which the actual signal was determined. The noise was then defined as the standard deviation of the residuals between the best-fit line and the values at individual pixels. The signal was defined as the difference between the best-fit line and the actual data value of a particular pixel. Once again, the effect of using different pixel ranges, from 1 to 13 pixels, as an integrated signal value was examined.

The software required for data processing was supplied with the spectrometer. Solutions of 0.01, 0.05, 0.1, 0.5, 1, 5, 10, 50, and 100 μg/ml of molybdenum were used to obtain data for detection limits, linearity, and dynamic range. Detection limits calculated on the basis of the

sideband-noise definition represent the average of those obtained from solutions having a molybdenum concentration within one to two orders of magnitude of the determined detection limit.

The third method for defining noise was more empirical but practical in nature and was used as a standard against which the other definitions could be evaluated. This method (see Fig. 5d) involved determining a peak-to-peak value for the noise surrounding each spectral line.

$$\text{Noise}_{(\text{peak-peak})} = 5\sigma \qquad (2)$$

The noise was evaluated at signal levels which were within approximately one order of magnitude of the detection limit. The standard definition of the detection limit (Eqn. 1) was then used to ascertain a detection-limit value. In essence, these empirical detection limits indicate where a signal peak begins to disappear into the baseline noise and serve as a convenient *de facto* standard.

Reagents

A 1000 μg/ml standard stock solution of molybdenum (Aldrich Chemical Company, Inc.) was used for preparation of the molybdenum dilutions used in this study. The standard solution was prepared by dissolving $(NH_4)_6Mo_7O_{24}$ in water. The standard solution was appropriately diluted with distilled and deionized water and stored in precleaned polypropylene containers (Nalgene).

RESULTS

Detection limits

In the foregoing discussion, the signal was defined as a peak area, A, while the noise was taken simply as the standard deviation of the residuals of the sideband pixels, σ. However, if the background noise is random, i.e. normally distributed, the standard deviation of the sum of n pixels should be $\sigma n^{1/2}$; that is, because the noise on individual pixels is random, it adds quadratically. Accordingly, if the peak signal area is obtained as a summation of n pixels, the proper sideband noise to employ in assigning a detection limit is $\sigma n^{1/2}$. Therefore,

$$DL_{(side)} = [Mo](3\sigma/A)(n)^{1/2} \qquad (3)$$

where [Mo] is the concentration of molybdenum resulting in the defined signal peak area A.

The consistency in detection limits that are based upon sideband noise (see Tables III and IV) for peak areas including 3-13 pixels is an indication of the general applicability of this sideband definition of the detection limit. In every case, the use of a single pixel for the determination of the sideband detection limit results in a value significantly different from the value obtained using 3-13 pixels.

The detection limits obtained for peaks 1-4 and peaks 5-10 (see peak designations in Table I) are listed in Tables III and IV, respectively. Figures 6 and 7 show examples of the signals at different integration periods for peaks 1- 4 and for peaks 5-10. No empirical detection limits are given in Table IV for those peaks (i.e. peaks 5, 6, 8, and 9) which were surrounded by interfering spectral lines, since the empirical detection limit obtained in such a situation would be unrealistically high.

The results compiled in Tables III and IV show that detection limits based upon the normalized sideband noise are more consistent with empirical values than are those based upon the background noise. For example, detection limits based upon background noise tend to increase as

the number of pixels used in the peak definition is raised. Additionally, for peaks 1, 7 and 10, as the integration time is increased from 10 to 100 seconds, the background-based detection limit increases whereas the empirical detection limit is lowered (as would be anticipated). Significantly, peaks 1, 7, and 10 all appear at positions on the photodiode array that is dominated by strong background emission (see Fig. 2c). The consistency of detection limits obtained using the sideband definition of noise, where the background emission is high, indicates the importance of the multiplex advantage in the photodiode-array spectrometer.

As would be expected, background-based and sideband detection limits for peaks 1, 2, 3, 4, 7, and 10 improve as the integration time is raised from 10 to 100 seconds. However, significant improvements in the empirical detection limit are not observed as the integration time is increased from 50 to 100 seconds. Generally, where background emission is very low (i.e. peaks 2-4) significant gains in signal-to-noise ratio can be obtained by the use of integration times as long as 100 seconds.

Consistently, the best values for sideband-based detection limits are derived for peak integrals obtained from five pixels. Because of the number, spectral range, and the variety (ionic and atomic) of peaks used in this study, we feel that this conclusion can be generalized to include peaks from other elements, even under circumstances where the signal is in a region dominated by background emission.

Linearity and dynamic range

Table V shows the results obtained for linearity and dynamic range for peaks 2, 3, and 4. Similar results were obtained for peaks 1 and 5-10. The fact that the slope values reported for the 100-second integration period differ from the slope values reported for the 10-second integration period by a factor other than 10 indicates that the instrument response is slightly different for these two integration periods. The linear dynamic range of a single integration time is approximately three orders of magnitude. If integration periods of 10 and 100 seconds are used, the dynamic

range of the instrument covers an additional order of magnitude. However, accuracy is best when the instrument is calibrated individually for each integration period.

Precision

Table VI shows the precision of the instrument reported for all 10 peaks at a molybdenum concentration of 0.5 µg/ml. The values were obtained with a 50-second integration time and are based upon a peak definition of 5 pixels. Sideband baseline correction was used. The data were collected over a period of 1.5 hours. The reported precision for peaks 2, 3, and 4 (3-4 %) is significantly better than that for peaks 1 and 5 (8%) and for peaks 6-10 (14-20%). The deterioration in precision for peak 1 and for peaks 5-10 can be attributed to the complex background emission observed in these regions of the photodiode array (see Figures 2 and 6). The lower precision observed for peaks located on the photodiode array at channels above 500 (peaks 6-10) arises because our prototype spectrometer is significantly less sensitive for emission signals occurring in this region (see Figure 3).

DISCUSSION

The ability of a multichannel spectrometer to monitor simultaneously both the signal and the sideband background offers the capability to correct for low-frequency fluctuations in background emission. In this sense, such a spectrometer offers a distinct advantage over single-channel photomultiplier-based systems.

When detection limits are determined with a multichannel spectrometer, the best definition of noise involves measuring the pixel-to-pixel fluctuations in background on each side of the spectral line. The signal definition which empirically provides the highest signal-to-noise ratio is derived from integrating a range of five pixels centered at the spectral peak. If such a peak area is employed, the noise must be normalized a factor of $(n)^{1/2}$, where n is the number of pixels (five, here) in the peak-area definition. This definition of noise results in detection limits which are similar to those obtained by empirical methods.

The linearity of the spectrometer extends over three orders of magnitude for a single integration period of 100 seconds. Linearity can be extended to at least four orders of magnitude by using additional integration times. However, when multiple integration periods are employed, each period must be calibrated independently.

Attainable precision is dependent upon the level of background emission; in instances where background emission is relatively low, a precision of about 3-4% can be expected for an integration period of 50 seconds (0.5 µg/ml Mo).

ACKNOWLEDGMENTS

Financial support by LECO Corporation, the National Science Foundation through grant CHE 87-22639, and by the Office of Naval Research is gratefully acknowledged. One of the authors (N.F.) wishes to thank the Science and Technology Foundation of Shimadzu for the grant of a travel fellowship. The authors are grateful to Dr. Scott W. McGeorge for his assistance in the preparation of software used in this study.

REFERENCES

1.) N.G. Howell and G.H. Morrison, *Anal. Chem.* 1977, **49**, 106.

2.) Y. Talmi, *Appl. Spectrosc.* 1982, **36**, 1.

3.) P.M. Epperson, J.V. Sweedler, R.B. Bilhorn, G.R. Sims, and M.B. Denton, *Anal. Chem.* 1988, **60**, 327A.

4.) Y. Talmi and R.W. Simpson, *Appl. Opt.* 1980, **19**, 1401.

5.) S.W. McGeorge, *Spectroscopy* 1987, **2(4)**, 106.

6.) G.M. Levy, A. Quaglia, R.E. Lazure, and S.W. McGeorge, *Spectrochim. Acta* 1987, **42B**, 106.

7.) V. Karanossios and G. Horlick, *Appl. Spectrosc.* 1986, **40**, 106.

8.) S.W. McGeorge, personal communication 1988.

Table I. Peak specifications for peaks 1-10 (see Figure 2).

Peak[a] Number	Spectral Line	Wavelength (nm)	Echelle Order	Dispersion (pm/mm)	Resolution[b] (pm)
1	Mo I	386.411	147	106.7	8.6
2	Mo II	287.151	198	79.2	8.8
3	Mo II	281.615	202	77.6	9.0
4	Mo II	277.540	205	76.5	8.1
5	Mo II	284.823	200	78.4	8.4
6	Mo I	379.825	150	104.5	10.0
7	Mo II	390.296	146	107.4	9.4
8	Mo II	263.876	216	72.6	7.6
9	Mo II	292.339	195	80.4	9.1
10	Mo I	313.259	182	86.2	9.7

a) Peaks refer to designations on spectrum in Figure 2d.
b) Calculated as full width at half maximum

Table II. Instrumental Parameters Optimized for Mo II Emission

Plasma forward power:	1.9 kW
Gas flow rates	
Outer:	16.0 l/min
Intermediate:	0.5 l/min
Inner (carrier):	0.9 l/min
Sample delivery rate:	1.6 ml/min
Observation height:	20 mm above the load coil
Magnification of ICP image:	1
Prepolychromator	
Entrance slit width:	25 mm
Entrance slit height:	5 mm
Photodiode array detector (1024 channels)	
Temperature:	-40^{o} C

Table III. Detection limits (ng/ml) for peaks 1-4.

Num. of Pixels[a] (n)	Detection Limit (ng/ml)											
	Peak 1 Mo I (386.411)			Peak 2 Mo II (287.151)			Peak 3 Mo II (281.615)			Peak 4 Mo II (277.540)		
	Emp.[b]	Backg.[c]	Side[d]	Emp.	Backg.	Side	Emp.	Backg.	Side	Emp.	Backg.	Side
	10 Second Integration											
1	91	164	98	28	61	39	26	52	20	68	112	42
3		116	66		49	25		49	13		54	27
5		125	67		60	22		54	11		65	25
7		158	71		70	23		56	12		62	26
9		206	76		74	24		66	12		92	26
11		221	82		83	25		68	13		98	28
13		245	87		94	26		79	14		89	29
	30 Second Integration											
1	62	47	50	19	36	18	24	33	22	29	47	33
3		40	36		40	12		23	14		44	21
5		56	36		48	11		26	13		59	20
7		79	38		56	11		26	13		69	20
9		74	41		62	11		32	13		80	21
11		93	44		72	12		37	14		97	22
13		110	46		79	13		41	15		114	24
	50 Second Integration											
1	43	88	41	11	35	19	7	26	14	16	27	27
3		93	29		35	13		27	9		24	17
5		115	29		44	12		29	8		36	16
7		133	31		49	12		33	8		39	16
9		154	33		56	12		33	9		44	17
11		163	35		63	13		37	9		48	18
13		173	37		65	14		39	10		52	19
	100 Second Integration											
1	33	138	31	12	32	10	7	21	11	18	34	14
3		173	21		36	6		23	7		35	9
5		219	22		42	6		24	6		41	8
7		282	23		47	6		25	7		49	9
9		334	25		51	6		27	7		61	9
11		320	26		54	7		30	7		77	10
13		250	27		61	7		32	8		90	10

a) Number of pixels used in determining both signal integral and blank (background) noise
b) Empirical-based detection limit
c) Background-based detection limit
d) Sideband-based detection limit

Table IV. Detection limits (ng/ml) for peaks 5-10.

Num. of Pixels[a] (n)	Detection Limit (ng/ml)														
	Peak 5 Mo II (284.823)		Peak 6 Mo I (379.825)		Peak 7 Mo II (390.296)			Peak 8 Mo II (263.876)		Peak 9 Mo II (292.339)		Peak 10 Mo I (313.259)		
	Emp.[b]	Side[d]	Emp.	Side	Emp.	Backg.[c]	Side	Emp.	Side	Emp.	Side	Emp.	Backg.	Side
10 Second Integration														
1	145	104	147	217	154	267	306	572	358	281	368	204	507	191
3	97	66	145	146		347	208	458	225	275	230		456	122
5	85	59	199	141		302	203	497	199	326	211		411	111
7	94	60	228	148		344	212	523	200	351	215		462	111
9	102	63	221	159		436	225	647	212	416	228		481	115
11	95	67	256	171		524	240	808	228	451	246		665	122
13	108	72	309	183		590	255	864	243	560	267		774	130
30 Second Integration														
1	66	35	239	124	74	486	108	363	168	238	168	121	416	182
3	59	23	200	86		458	76	310	105	201	105		336	121
5	75	21	186	83		480	76	363	96	216	98		300	109
7	88	21	170	86		527	80	385	98	232	100		312	109
9	98	22	153	90		567	85	475	103	262	105		384	112
11	113	24	198	95		616	90	557	109	263	111		453	118
13	131	25	222	101		731	95	669	116	280	119		533	125
50 Second Integration														
1	57	19	149	51	68	327	60	187	246	147	187	57	403	101
3	51	12	198	35		345	43	194	158	142	121		300	65
5	59	11	196	34		279	42	220	145	154	112		237	59
7	66	12	179	36		298	45	284	149	163	115		227	59
9	81	12	280	38		311	47	331	158	189	122		243	61
11	93	13	392	40		345	50	384	169	223	130		265	64
13	104	14	427	42		403	53	441	180	279	138		303	68
100 Second Integration														
1	62	39	514	119	46	635	50	264	306	326	290	50	941	88
3	64	25	364	80		705	34	316	195	245	183		840	56
5	71	24	127	78		720	33	420	180	167	166		730	51
7	84	24	571	84		661	35	525	186	235	169		679	52
9	93	26	1334	92		659	37	576	196	478	181		779	54
11	103	28	2021	100		843	39	627	207	814	193		953	57
13	119	31	2268	108		1113	41	731	220	1277	208		1085	60

a) Number of pixels used in determining both signal integral and blank (background) noise
b) Empirical-based detection limit
c) Background-based detection limit
c) Sideband-based detection limit

Table V. Linearity and linear dynamic range of blank-corrected peak areas obtained from five pixels.

	Peak 2		Peak 3		Peak 4	
Integration Time (sec)	10	100	10	100	10	100
Linear Dynamic Range (μg/ml)	0.05 - 100	0.01 - 10	0.05 - 100	0.01 - 10	0.5 - 100	0.05 - 10
Slope ± σ	263.6 ± 0.8	2347 ± 4	396.0 ± 0.5	3437 ± 8	184.0 ± 0.6	1590 ± 2
y-intercept ± σ	–40 ± 30	10 ± 20	-40 ± 20	-20 ± 30	-40.0 ± 30	0 ± 10
Correlation Coefficient (r)	1.000	1.000	1.000	1.000	1.000	1.000

Table VI. Precision for a signal definition of 5 pixels.

Peak Number	Wavelength (nm)	Precision (%R.S.D.)
1	386.411	7.77
2	287.151	3.98
3	281.615	2.73
4	277.540	3.75
5	284.823	7.59
6	379.825	16.96
7	390.296	14.34
8	263.876	15.22
9	292.339	14.02
10	313.259	19.61

FIGURE CAPTIONS

Figure 1 Schematic diagram of the Plasmarray spectrometer.

Figure 2 Spectra obtained from the photodiode array; 10-second integration, vertical scales are identical in all spectra. Mo peaks identified in Table I.

a) dark current
b) dark-current-subtracted blank spectrum
c) dark-current-subtracted sample spectrum from 5 μg/ml molybdenum solution
d) blank-subtracted Mo spectrum (spectrum c - spectrum b)

Figure 3 Relative efficiency of the prototype spectrometer used in the present study. This spectrum was obtained by removing the optical mask from the spectrometer and by monitoring ICP background emission.

Figure 4 Spectra obtained under optimized operating conditions for a) atomic emission and b) ionic emission. Optimized conditions for atomic emission: plasma forward power, 1.1 kW; sample delivery rate, 1.0 ml/min. All other parameters were the same as the optimized conditions for ionic emission, listed in Table II. Spectral lines are identified in Table I; peaks 1, 6, and 10 arise from the neutral atom while all other numbered peaks correspond to Mo ion lines.

Figure 5 Signal definitions for:

a) Dark-subtracted blank trace illustrating the procedure for obtaining noise for the background-based detection limit. The noise was defined as the standard deviation of the peak areas obtained for 10 blank determinations. The number of pixels integrated for the total signal was varied.
b) Blank-subtracted peak illustrating the procedure for defining the signal for the background-based detection limit. A best-fit line was obtained from selected regions in the sideband background. The signal was defined as the summation of the difference values between the signal and the best-fit line. The number of pixels integrated for the total signal was varied.
c) Blank-subtracted peak illustrating the procedure for defining the signal and noise for the sideband-based detection limit. The noise was defined as the standard deviation of the pixel values in the defined sideband regions. The signal was defined in the same manner as in b.
d) Blank-subtracted peak illustrating the procedure for defining the signal and noise for the empirically-based detection limit. The peak-to-peak pixel values of the surrounding sideband regions was defined as being equal to 5σ. The signal was defined as a peak height above a best-fit line which was obtained from the surrounding sideband regions.

Figure 6 Spectra obtained for peaks 1-4 using signal-integration periods of a) 10 seconds, b) 30 seconds, c) 50 seconds and d) 100 seconds. The molybdenum concentration was 100 ng/ml.

Figure 7 Spectra obtained for peaks 5-10 using signal integration periods of a) 10 seconds, b) 30 seconds, c) 50 seconds and d) 100 seconds. The molybdenum concentration was 500 ng/ml.

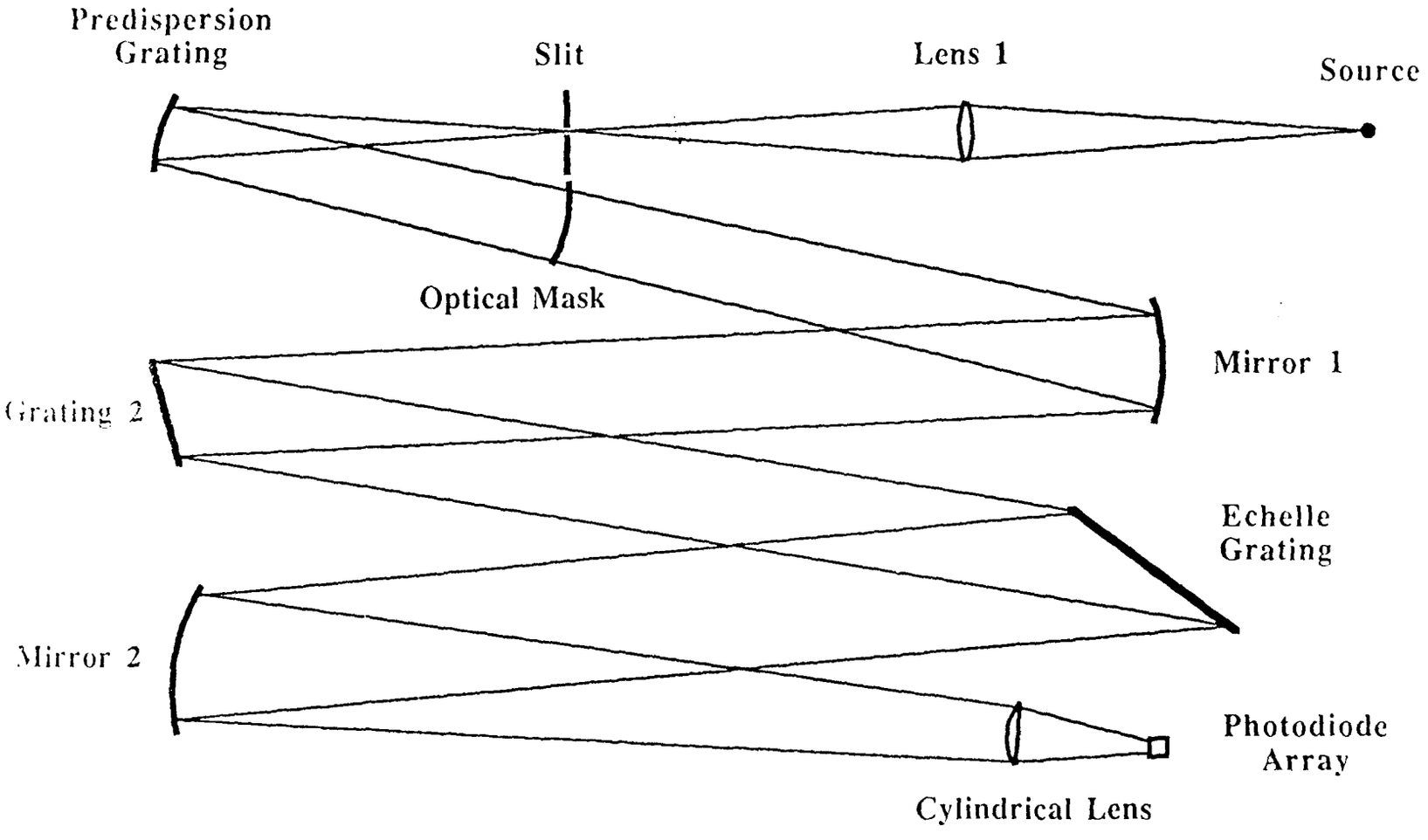
Predispersion Grating
Slit
Lens 1
Source
Optical Mask
Mirror 1
Grating 2
Echelle Grating
Mirror 2
Photodiode Array
Cylindrical Lens

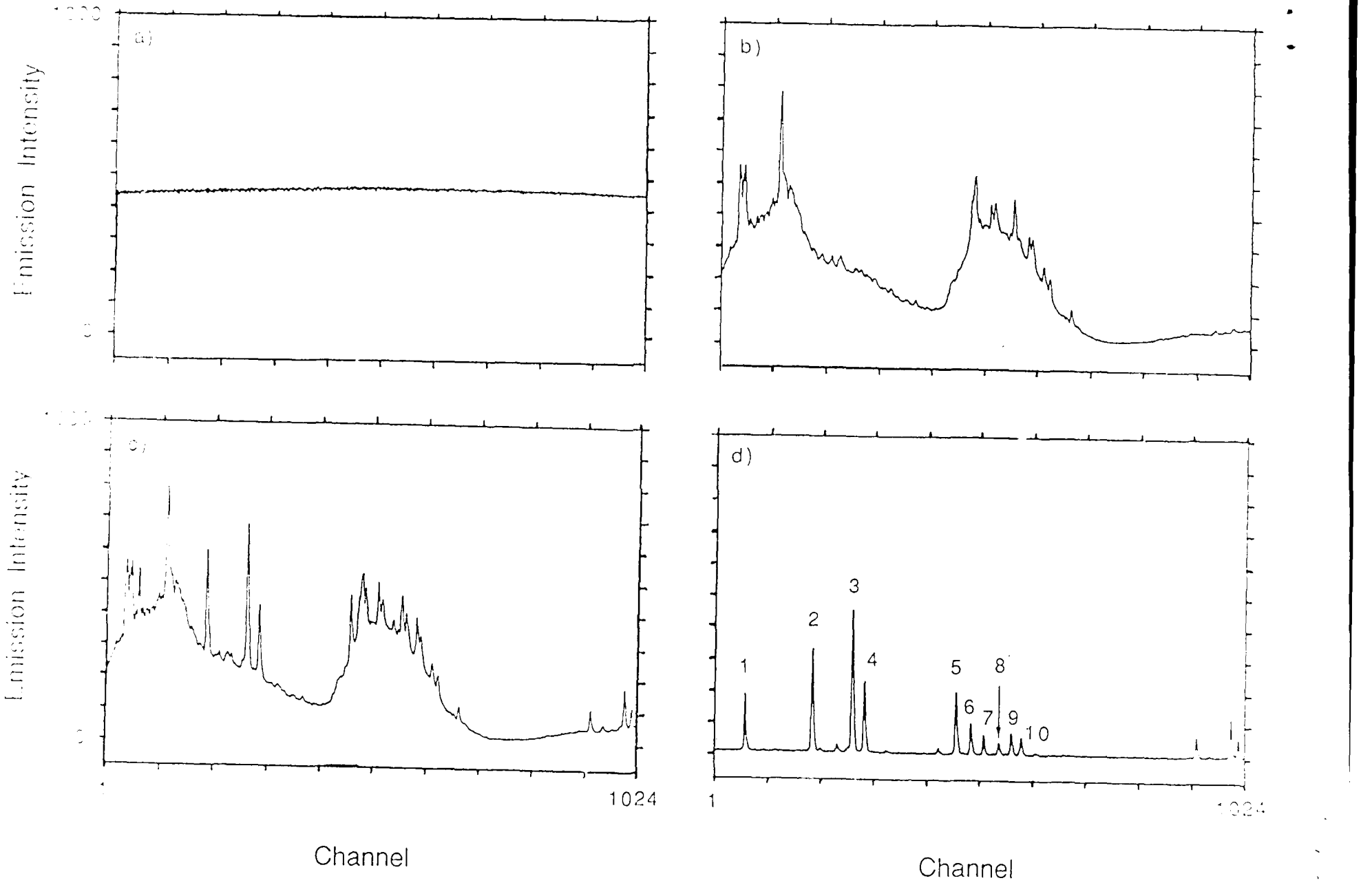
a)
b)
c)
d)
Emission Intensity
Emission Intensity
1
1024
Channel
Channel
1
2
3
4
5
6
7
8
9
10

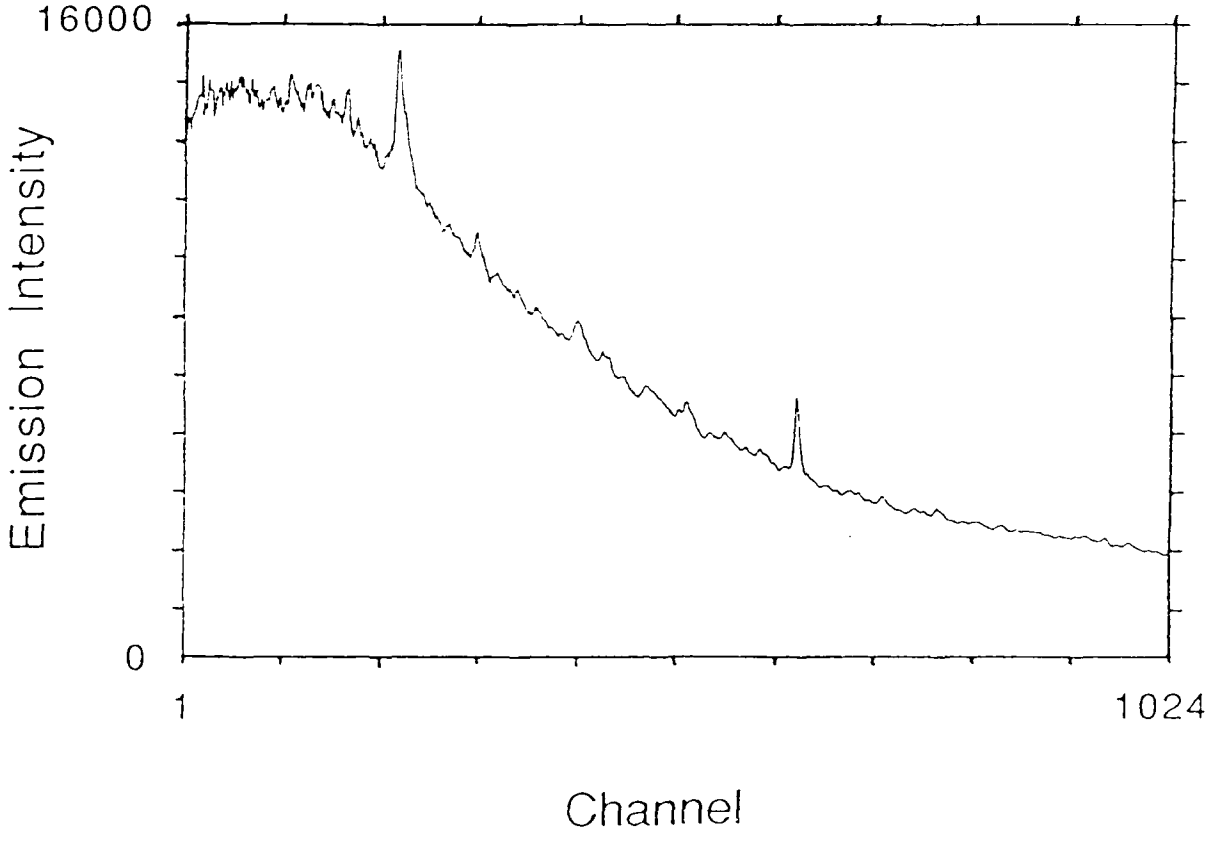
16000
Emission Intensity
0
1
1024
Channel

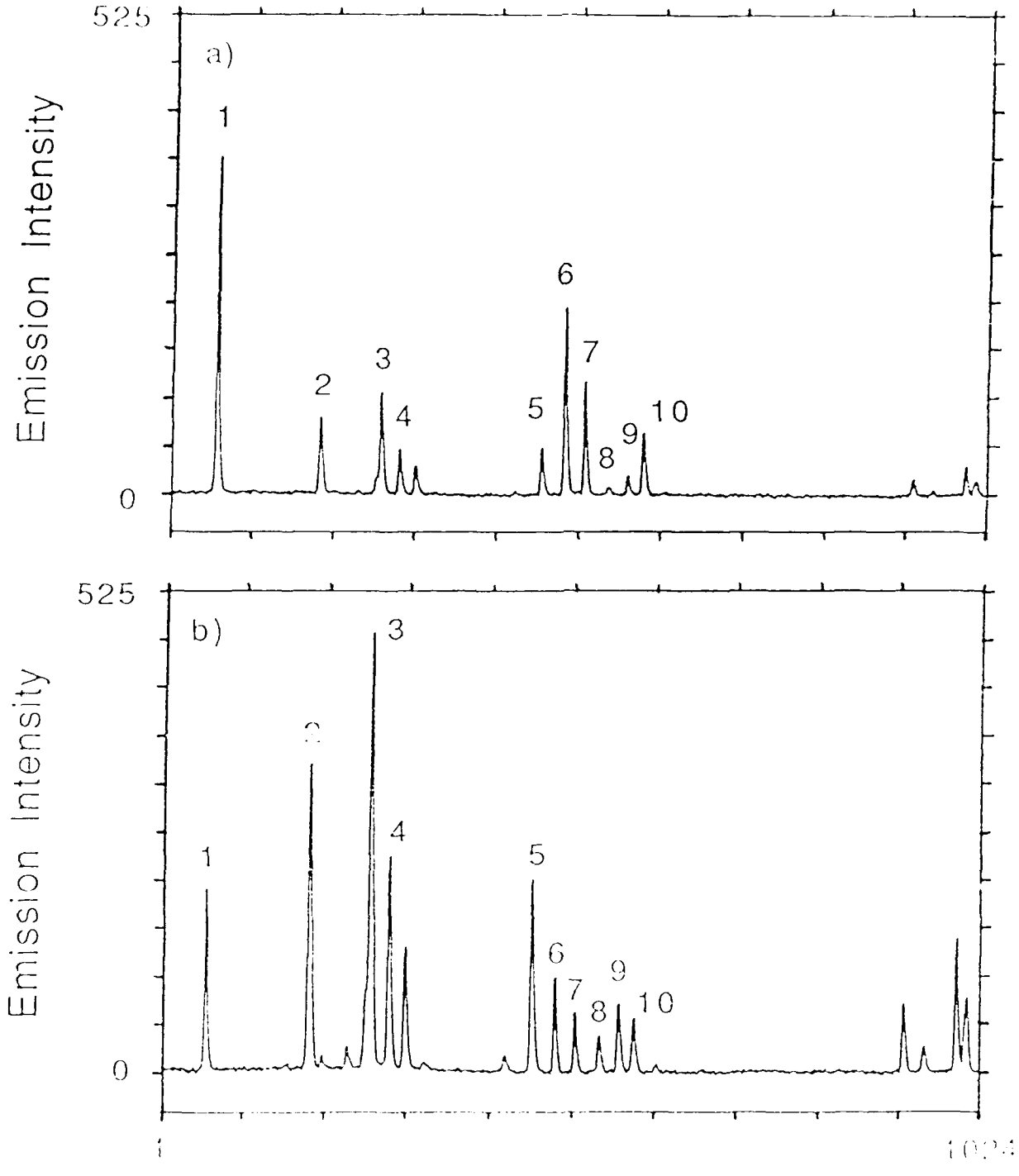
525
a)
Emission Intensity
1
2
3
4
5
6
7
8
9
10
0
525
b)
Emission Intensity
1
2
3
4
5
6
7
8
9
10
0
1
1024

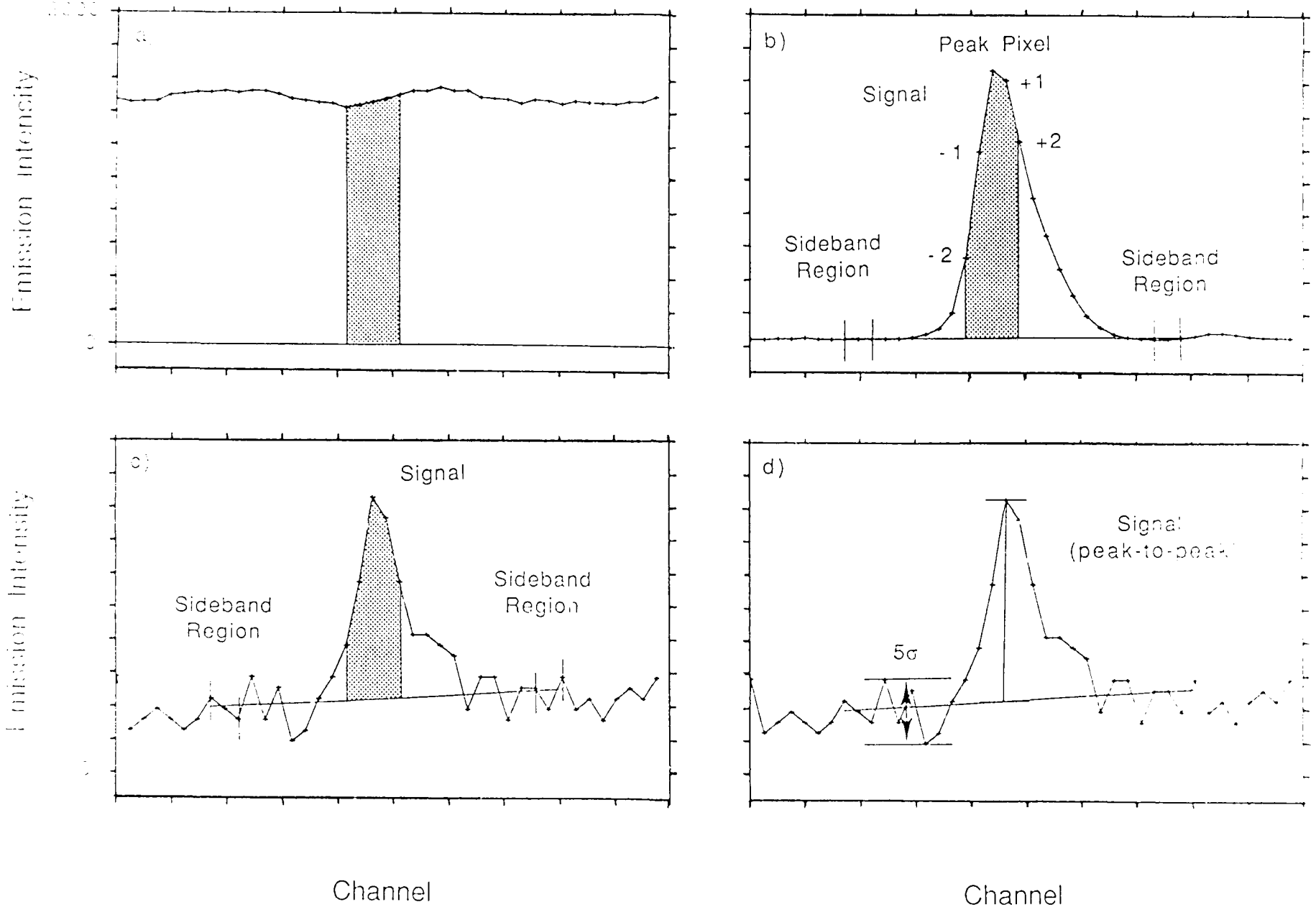
a)
b)
Peak Pixel
Signal
+1
+2
-1
-2
Sideband
Region
Sideband
Region
c)
Signal
Sideband
Region
Sideband
Region
d)
Signal
(peak-to-peak)
5σ
Emission Intensity
Emission Intensity
Channel
Channel

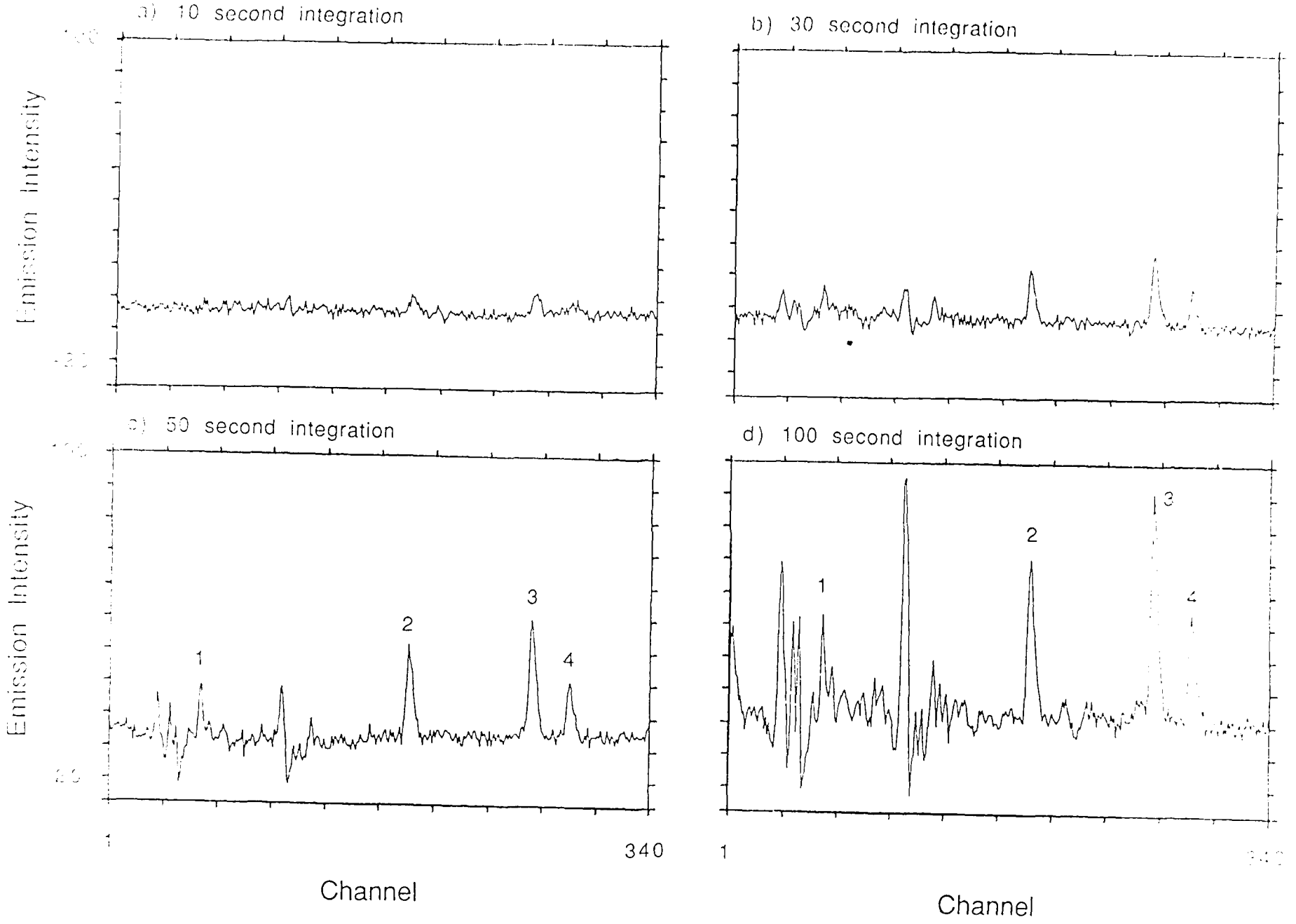
a) 10 second integration
b) 30 second integration
c) 50 second integration
d) 100 second integration
Emission Intensity
Emission Intensity
1
2
3
4
1
340
Channel
Channel

Figure 2

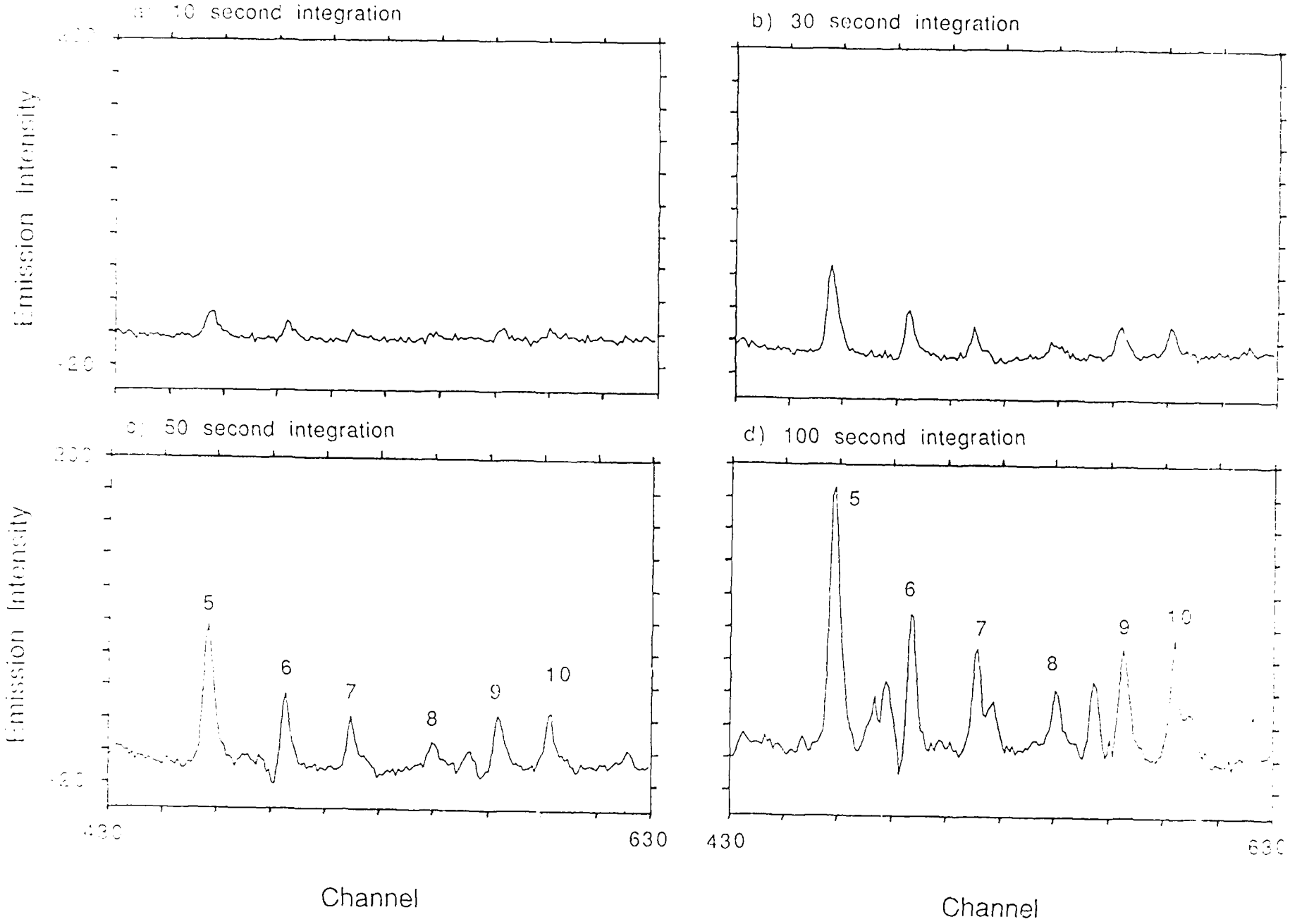
a) 10 second integration
b) 30 second integration
c) 50 second integration
d) 100 second integration
Emission Intensity
Emission Intensity
5
6
7
8
9
10
5
6
7
8
9
10
430
630
430
630
Channel
Channel